

# Interaction of Peroxyformic Acid with Water Molecules: A First-Principles Study

Anant D. Kulkarni,<sup>\*,†</sup> Dhurba Rai,<sup>‡</sup> Libero J. Bartolotti,<sup>§</sup> and Rajeev K. Pathak<sup>\*,‡</sup>

Department of Chemistry, University of Pune, Pune 411 007, India, Department of Physics, University of Pune, Pune 411 007, India, and Department of Chemistry, East Carolina University, Science and Technology Building, Suite 300, Greenville, North Carolina 27858-4353

Received: July 3, 2006; In Final Form: August 23, 2006

The present article comprises a theoretical study of structures and energetics of the lowest energy conformers of peroxyformic acid (PFA) and its hydrated variants, viz.  $\text{PFA}\cdots(\text{H}_2\text{O})_n$  ( $n = 1-4$ ), at the molecular level. We have employed two different ab initio quantum chemical methods, viz. restricted Hartree–Fock (RHF) and the second-order Møller–Plesset (MP2) perturbation theory with the basis sets 6-31G(d,p) and 6-311++G-(2d,2p). Modifications in the structure as well as vibrational frequencies of PFA brought about by successive addition of  $\text{H}_2\text{O}$  molecules are also discussed. Cooperativity of hydrogen bonding in these clusters can be gauged through a detailed many body interaction energy analysis.

## I. Introduction

Mono- or disubstituted derivatives ( $\text{ROOR}'$ ) of hydrogen peroxide, by virtue of a wide range of reactions brought about by them, are of great interest in synthetic organic chemistry.<sup>1–16</sup> Among this class of compounds, peracids, i.e., acids in which the acidic  $-\text{OH}$  group is replaced by an  $-\text{OOH}$  group (from peroxide), form by themselves a class of reactants in synthetic organic chemistry. Peracids play a vital role in several chemically important reactions such as oxidizing agents in the epoxidation type of reactions where a carbon–carbon double bond in alkenes undergoes oxidation to generate epoxides (oxiranes), as a reagent in Baeyer–Villiger oxidation<sup>12</sup> type of reactions, and so forth. Some of these acids are peroxycarboxylic acids, such as peroxyformic acid (also called performic acid) and *m*-chloroperoxybenzoic acid (*m*CPBA). Performic acid (PFA), a planar molecule ( $\text{HC}(:\text{O})\text{OOH}$ ), manifests itself in *cis* and *trans* forms (as discussed in section II). For an isolated PFA molecule, the *cis* form (electrical dipole moment (experimental) = 1.39 D),<sup>3</sup> exhibits a greater stability than its *trans* counterpart and is endowed with a low activation barrier for undergoing a reaction. Moreover, the *cis* form shows a striking feature of an *intramolecular* hydrogen bond.<sup>3</sup> Recent literature reveals several studies on chemical reactions involving peracids as one of the reactants. In particular, the hydrogen-bonded complexes of peracids constitute a fascinating area that is studied extensively employing experimental and theoretical techniques, as highlighted below.<sup>5–16</sup>

An earlier study, in 1947, on the application of performic acid for oxidation of insulin was reported by Sanger.<sup>4</sup> Recently, Langley and Noe<sup>5</sup> have performed ab initio studies of the conformations of performic acid, peracetic acid, and methyl performate at Hartree–Fock (HF) and Møller–Plesset second-order perturbation (MP2) levels using various basis sets. The lowest energy conformers of performic acid and peracetic acid are both eclipsing about the O–O bond with planar ( $C_s$ )

geometries. This conformation is stabilized by internal hydrogen bonding between the OH hydrogen and the carbonyl oxygen. Anderson and Carter<sup>6</sup> employed density functional theory (DFT) to delve into pathways for combustion of dimethyl ether at low temperature. Along with the energetics of the reactions, these authors also discussed the possible role of the Criegee intermediate in the combustion reaction where PFA is one of the intermediate reactants.

There exist several studies on epoxidation by peracids<sup>7</sup> as evidenced by the following significant works: (1) Epoxidation mechanisms of alkenes by peroxy acids were reported by Okovytyy, Gorb, and Leszczynski,<sup>7</sup> who investigated the transition state structure for the reaction of the epoxidation of ethylene with peroxyformic acid at the CASSCF and UQCISD levels of theory. Both these methods predict<sup>7</sup> the existence of a highly unsymmetrical oxygen-addition transition state with a diradical character. The estimated value of the activation barrier at the MCQDPT2(12,12)/6-311++G(d,p)//CASSCF(12,12)/6-311++G(d,p) correlated level is 18.3 kcal mol<sup>-1</sup>, which is in consonance with experimental findings. (2) Theoretical study of olefinic epoxidation by peracids was carried out by Yamabe et al.<sup>8</sup> for the parent reacting system  $\text{HCOOOH} + \text{CH}_2:\text{CH}_2 \rightarrow \text{HCOOH} + \text{C}_2\text{H}_4\text{O}$ . The potential energy surface was determined employing ab initio methods whence the existence of the oxygen-addition transition state was confirmed by experiments. This transition state evolves into a hydrogen-bonded system (ethylene oxide and formic acid) via an intermediate. According to this study, while the substituent effects on transition state geometries were small, the activation energy effects turn out to be fairly large. (3) Computations at the density functional level (with the B3LYP prescription) using the 6-311+G(d,p) basis set were reported by Freccero et al.,<sup>9</sup> who investigated the mechanisms for epoxidation of norbornene, norbornadiene, and tetramethylethene, as well as *anti*- and *syn*-sesquinorbornenes, by peroxyformic acid. The computed data obtained can be employed to reproduce the experimental facial syn selectivity of norbornene and norbornadiene epoxidations and also compare well with the experimental activation free energies of the peroxy acid epoxidation of all the olefins, validating the adequacy of the method employed.

\* Corresponding authors. E-mail: anantkul@chem.unipune.ernet.in (A.D.K.); pathak@physics.unipune.ernet.in (R.K.P.).

<sup>†</sup> Department of Chemistry, University of Pune.

<sup>‡</sup> Department of Physics, University of Pune.

<sup>§</sup> East Carolina University.

The internal rotation in performic acid is a salient feature that has also been studied in its different facets. An earlier study reporting the theoretical findings of internal rotation in peroxyformic acid was carried out by Carlo.<sup>13</sup> In this work the SCF MO LCAO method was used with the STO-3G and 4-31G basis sets using experimental and optimum values of the geometrical parameters. Both these basis sets yielded a flat-double-minimum potential for the CO–OH torsion, leading to the planar (trans) form being slightly preferred in comparison with the cis one; however, improved basis sets deem that the cis version has greater stability, as pointed out above. This study also attempted to explain the effects of substitution in PFA on the internal rotation. Recently, significant contributions to the area of theoretical study of PFA chemistry were made by Bach, Estevez, Winter, and Glukhovtsev.<sup>11</sup> They carefully explored the origin of substrate directional effects in the epoxidation of allyl alcohols using performic acid. In this study, the reactant cluster and transition state for epoxidation of allyl alcohol with PFA were obtained at the MP2/6-31G(d) level of theory. Interestingly, the activation parameters of the reaction calculated at the B3LYP/6-311G(d,p) level are in excellent agreement with their corresponding MP4//MP2 level values. The directional effect of the hydroxyl group in the transition state is attributed initially to a primary hydrogen bonding interaction between the relatively more acidic peroxy acid proton and the oxygen of the allyl alcohol. Bach, Willis, and Langley<sup>5,14</sup> in another theoretical study determined that the C–O and O–O barriers were 7.68 and 1.04 kcal/mol, respectively. The relatively low O–O barrier is a consequence of a balance between electron repulsion and hydrogen bonding in the syn chelated conformer. In their extensive pursuit of reactions participated in by PFA, Bach et al. characterized binding and reactivity; some of their studies are summarized here. Bach and Dmitrenko,<sup>15</sup> through their high-level ab initio and CASSCF calculations, studied the transition structure (TS) epoxidation of ethylene by protonated peroxyformic acid. The main objective of their work had been to distinguish between a spiro vis-à-vis a planar orientation of the peracid. According to their study the planar TS is 11.5 kcal/mol higher in energy than an unsymmetric spiro TS. Additional computations at CASSCF and DFT levels also favor the spiro TS. The ab initio study of the influence of substituents and intramolecular hydrogen bonding on the carbonyl bond length and stretching force constant in monosubstituted carbonyl compounds was reported by Bock, Trachtman, and George.<sup>16</sup> According to this ab initio study with a 4-31G basis set, not only does the atom directly bonded to the carbonyl C affect the magnitude of equilibrium bond lengths and the force constants, but the rest of the substituent group is capable of exerting an even greater influence.

The foregoing discussion brings out the versatility of PFA as a strong oxidant. Notably, most of these reactions occur in aqueous ambience. It is well-known that the oxidation brought about by hydrogen peroxide, H<sub>2</sub>O<sub>2</sub>, is particularly enhanced in aqueous medium.<sup>19</sup> It would therefore be instructive to study the complexes formed between peroxyformic acid (PFA) and water, viz. PFA⋯(H<sub>2</sub>O)<sub>n</sub>, on similar lines of peroxide–water systems.<sup>17,18,20–23</sup>

The present venture comprises a systematic theoretical study of PFA⋯(H<sub>2</sub>O)<sub>n</sub> (*n* = 1–4) complexes at ab initio quantum chemical level and the effect of these water molecules on the intramolecular hydrogen bond of PFA. This study is also aimed at providing, at the molecular level, a tool to understand the cooperativity in such complexes. We also study herein the PFA–water “structuring”/“destructuring” effect, the basis set

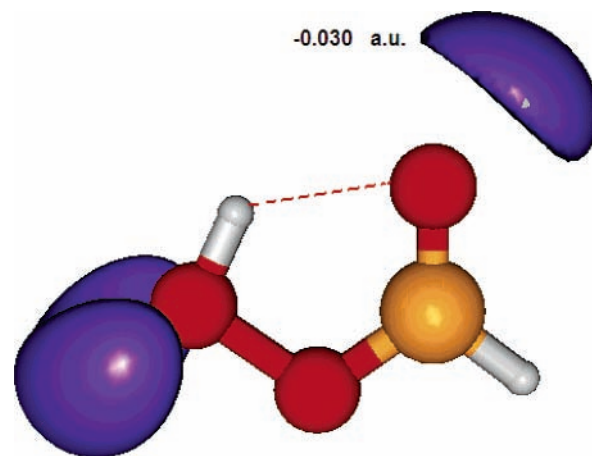


**Figure 1.** Molecular electrostatic potential (MESP) isosurface (isosurface value  $-0.030$  au) for PFA molecule computed at MP2/6-311++G(2d,2p) level optimized geometry. Refer to the text for further details.

effects, the trends in energetics, and basic building patterns and similarity patterns with (H<sub>2</sub>O)<sub>n</sub> clusters.

## II. Methodology

The structures of PFA⋯(H<sub>2</sub>O)<sub>n</sub> (*n* = 1–4) were generated essentially by a supermolecular approach,<sup>23,24</sup> augmented by the knowledge of the lowest energy clusters<sup>23,24</sup> of H<sub>2</sub>O<sub>2</sub>⋯(H<sub>2</sub>O)<sub>n</sub> and (H<sub>2</sub>O)<sub>n</sub>. For this purpose the cis form for PFA (energy  $-264.39832$  hartree at MP2/6-311++G(2d,2p); cf. Figure 1) was chosen since it is energetically more stable than its trans variant (energy  $-264.39292$  hartree at MP2/6-311++G(2d,-2p)). The geometry optimizations were accomplished through the Gaussian 03 suite of programs. All the computations were performed at RHF and MP2 levels employing a reliable basis set, viz. 6-31G(d,p) (which uses 25 and 70 basis functions for H<sub>2</sub>O and PFA, respectively), for initial structure generation and scanning of energetically favorable conformers. For accurate estimation of interaction energies and geometrical parameters, all the lowest energy structures were reoptimized at the MP2 level employing an extended basis set, 6-311++G(2d,2p) (“triple- $\zeta$ ” basis set augmented with diffuse and polarization functions, using 48 and 128 basis functions for water and PFA, respectively).

The energetically favorable clusters on the potential energy surface (PES) were selected from a scan of at least 25 structures for each *n* (*n* > 2) at the RHF/6-31G(d,p) level. These were chosen for follow-up at a higher level, viz. MP2, in conjunction with an improved basis set. Further, to reaffirm the minimum (at least, local) nature of these structures, we have performed vibrational frequency calculations at the MP2/6-311++G(2d,-2p) level.

The structure generation, visualization, and vibrational frequency analysis were carried out with the help of two versatile visualization packages, UNIVIS-2000<sup>28</sup> and MOLDEN.<sup>29</sup> Many body interaction energy analysis and incorporation of the basis set superposition error (BSSE) correction have been performed using the turnkey program MBAC developed by Kulkarni et al.,<sup>30</sup> in the spirit of the works by Elrod and Saykally<sup>31</sup> and Xantheas.<sup>32</sup>

## III. Results and Discussion

PFA⋯H<sub>2</sub>O complexes are generated from the knowledge of H<sub>2</sub>O<sub>2</sub>⋯H<sub>2</sub>O complexes and the cooperativity picture offered by a molecular electrostatic potential (MESP) isosurface map

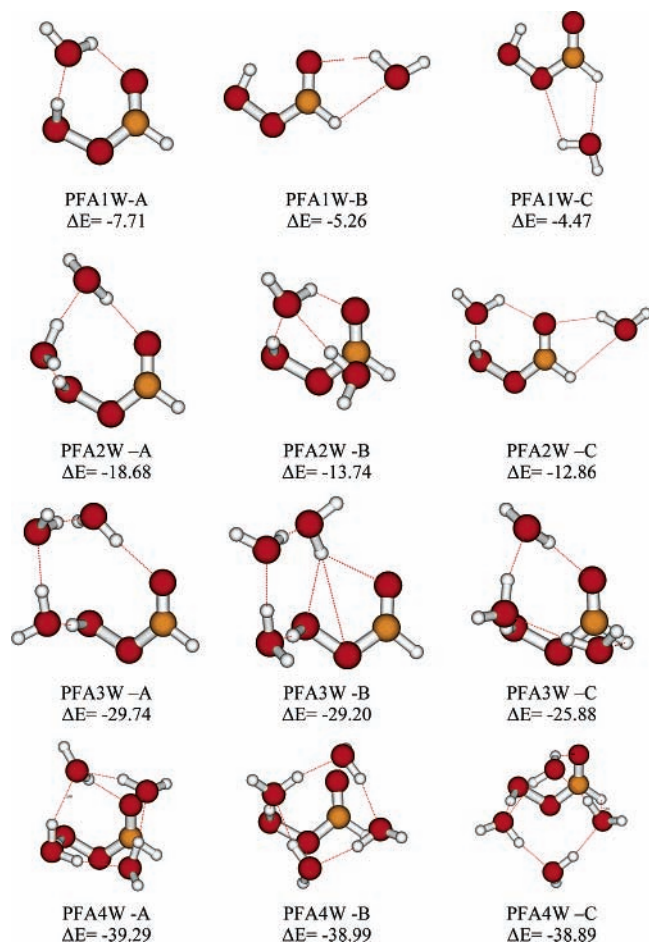


**Figure 2.** MP2/6-311++G(2d,2p) optimized structures of PFA...( $\text{H}_2\text{O}$ )<sub>n</sub>,  $n = 1-4$ , clusters along with the corresponding interaction energies in kcal mol<sup>-1</sup>.

of PFA (cf. Figure 1). From Figure 1, it is evident that the regions preponderant with a negative MESP would be conducive for hydrogens to bind. These negative potential regions occur in the vicinity around the oxygen atoms in the exterior, by virtue of the lone electron pairs. For the present study we have chosen the cis conformer of PFA, which is the most stable among the reported isolated conformers of PFA. The entire discussion of the PFA...( $\text{H}_2\text{O}$ )<sub>n</sub> clusters in the present article pertains to the MP2/6-311++G(2d,2p) level unless stated otherwise.

The most stable conformers of PFA...H<sub>2</sub>O are depicted in Figure 2 with the details of energetics given in Table 1. These conformers were chosen after a decent scan of at least 25 structures for each  $n$ . It may be seen from Table 1 that PFA1W-A has interaction energy  $-7.709$  kcal mol<sup>-1</sup>, with respect to its isolated monomer units, at the MP2/6-311++G(2d,2p) level (used throughout, unless otherwise indicated). It is observed from Figure 2 that all the PFA...H<sub>2</sub>O structures (viz. PFA1W-A, PFA1W-B, and PFA1W-C) have two hydrogen bonds each and possess interaction energies between  $-7.709$  and  $-4.471$  kcal mol<sup>-1</sup> at the MP2/6-311++G(2d,2p) level. For PFA1W-A, the interaction between PFA and H<sub>2</sub>O is stronger ( $-7.709$  kcal mol<sup>-1</sup>) than the H<sub>2</sub>O...H<sub>2</sub>O interaction ( $-5.365$  kcal mol<sup>-1</sup> in isolated water dimer) and that of the H<sub>2</sub>O<sub>2</sub>...H<sub>2</sub>O interaction<sup>23</sup> ( $-7.503$  kcal mol<sup>-1</sup>; the structure was reoptimized at the MP2/6-311++G(2d,2p) level of theory). Interestingly, the intramolecular hydrogen bond in PFA is not seen in PFA1W-A, whereas one cannot preclude its presence in PFA1W-B and PFA1W-C. The minimum energy clusters for PFA...H<sub>2</sub>O are employed as the starting guess for generating the higher clusters along with the other structures generated from the various other techniques (described in the Methodology section). Structures of PFA...( $\text{H}_2\text{O}$ )<sub>n</sub> for  $n = 2$  and 3, viz. PFA2W-A, PFA2W-B, PFA2W-C, PFA3W-A, PFA3W-B, and PFA3W-C (cf. Figure 2), may be interpreted to manifest via various possible combinations of lowest energy structures of PFA...H<sub>2</sub>O along with additional water molecule(s), all striving for maximal cooperativity. The interaction energy of PFA...( $\text{H}_2\text{O}$ )<sub>2</sub> clusters ranges from  $-18.679$  to  $-12.859$  kcal mol<sup>-1</sup>, whereas for PFA...( $\text{H}_2\text{O}$ )<sub>3</sub> clusters the range narrows to  $-29.203$  to  $-29.956$  kcal mol<sup>-1</sup>. The details of energetics at various levels are presented in Table 1. For three water molecules ( $n = 3$ ) binding with PFA, as depicted in Figure 2, the clusters evince diversified patterns with the ( $\text{H}_2\text{O}$ )<sub>2</sub> and distorted ( $\text{H}_2\text{O}$ )<sub>3</sub> as the basic building blocks (PFA3W-A and PFA3W-C) along with a tendency to form structures similar to ( $\text{H}_2\text{O}$ )<sub>4</sub> by forming the hydrogen bond with the O-H from PFA (PFA3W-B). The additional water molecules around PFA...( $\text{H}_2\text{O}$ )<sub>n</sub>,  $n = 3$  and 4, clusters has the tendency to manifest in patterns akin to ( $\text{H}_2\text{O}$ )<sub>4</sub> with PFA cooperativity, which also is reflected in the  $n = 4$  clusters, viz. PFA4W-A, PFA4W-B, and PFA4W-C (cf. Figure 2). There also are seen to exist several low-lying clusters for  $n = 3$  and 4 which may be generated, e.g., by flipping the covalent O-H bond, without diminishing cooperativity. Interestingly, this

**TABLE 1: Raw,<sup>a</sup> ZPE-Corrected, and BSSE-Corrected Interaction Energies (in kcal mol<sup>-1</sup>) of PFA...( $\text{H}_2\text{O}$ )<sub>n</sub> ( $n = 1-4$ ) Clusters at RHF and MP2 Levels Employing 6-31G(d,p) and 6-311++G(2d,2p) Basis Sets**

structure code	$\Delta E(\text{RHF/I})^b$	$\Delta E(\text{RHF/II})^c$	$\Delta E(\text{MP2/I})^d$	$\Delta E(\text{MP2/II})^e$	$\Delta E_{\text{ZPE-corr}}^f$	$\Delta E_{\text{BSSE-corr}}^g$	$\Delta E_{\text{ZPE+BSSE-corr}}^h$
PFA1W-A	-9.413	-6.339	-11.044	-7.709	-5.519	-6.025	-3.835
PFA1W-B	-5.308	-3.999	-6.625	-5.261	-3.752	-4.362	-2.852
PFA1W-C	-4.515	-3.266	-5.872	-4.471	-3.347	-3.672	-2.548
PFA2W-A	-20.257	-14.663	-24.924	-18.679	-14.682	-15.183	-11.186
PFA2W-B	-20.195	-10.217	-19.040	-13.741	-8.921	-10.677	-5.857
PFA2W-C	-14.324	-10.091	-17.543	-12.859	-9.067	-10.177	-6.385
PFA3W-A	-30.913	-22.585	-38.559	-29.203	-22.354	-24.368	-16.985
PFA3W-B	-27.263	-19.205	-34.461	-25.882	-21.920	-23.902	-16.619
PFA3W-C	-26.614	-19.255	-31.623	-23.956	-21.173	-20.754	-16.044
PFA4W-A	-40.849	-28.692	-53.358	-39.289	-29.269	-32.380	-22.360
PFA4W-B	-39.636	-27.637	-52.302	-38.986	-29.031	-31.473	-21.518
PFA4W-C	-39.578	-28.375	-52.056	-38.895	-28.931	-31.360	-21.395

<sup>a</sup> "Raw" interaction energies refer to energies not corrected for either ZPE and BSSE. <sup>b</sup>  $\Delta E(\text{RHF/I})$ : interaction energy at RHF/6-31G(d,p) optimized geometry. <sup>c</sup>  $\Delta E(\text{RHF/II})$ : interaction energy at RHF/6-311++G(2d,2p) optimized geometry. <sup>d</sup>  $\Delta E(\text{MP2/I})$ : interaction energy at MP2/6-31G(d,p) optimized geometry. <sup>e</sup>  $\Delta E(\text{MP2/II})$ : interaction energy at MP2/6-311++G(2d,2p) optimized geometry. <sup>f</sup>  $\Delta E_{\text{ZPE-corr}}$ : ZPE-corrected interaction energy at MP2/6-311++G(2d,2p) optimized geometry. <sup>g</sup>  $\Delta E_{\text{BSSE-corr}}$ : BSSE-corrected interaction energy at MP2/6-311++G(2d,2p) optimized geometry. <sup>h</sup>  $\Delta E_{\text{ZPE+BSSE-corr}}$ : ZPE- and BSSE-corrected interaction energy at MP2/II level optimized geometry.

**TABLE 2: Many Body Interaction Energy Analysis of PFA $\cdots$ (H $_2$ O) $_n$  ( $n = 2-4$ ) Clusters Performed at MP2/6-311++G(2d,2p) Level<sup>a</sup>**

molecular combinations involved and many body energy terms	energy contributions (kcal mol <sup>-1</sup> )
(A) PFA $\cdots$ (H $_2$ O) $_2$	
PFA $\cdots$ W1	-6.020
PFA $\cdots$ W2	-8.472
W1 $\cdots$ W2	-4.896
total 2-body energy	-19.388
total 2-body energy excluding ref mol	-4.896
PFA $\cdots$ W1 $\cdots$ W2 = total 3-body energy	-3.196
$E_R$	3.910
$\Delta E$	-18.673
(B) PFA $\cdots$ (H $_2$ O) $_3$	
PFA $\cdots$ W1	-2.539
PFA $\cdots$ W2	-8.358
PFA $\cdots$ W3	-5.347
W1 $\cdots$ W2	-4.808
W1 $\cdots$ W3	-4.844
W2 $\cdots$ W3	-1.654
total 2-body energy	-27.551
total 2-body energy excluding ref mol	-11.306
PFA $\cdots$ W1 $\cdots$ W2	-2.153
PFA $\cdots$ W1 $\cdots$ W3	-1.328
PFA $\cdots$ W2 $\cdots$ W3	-1.123
W1 $\cdots$ W2 $\cdots$ W3	-1.479
total 3-body energy	-6.083
$E_R$	4.508
$\Delta E$	-29.725
(C) PFA $\cdots$ (H $_2$ O) $_4$	
PFA $\cdots$ W1	-5.622
PFA $\cdots$ W2	-7.904
PFA $\cdots$ W3	-3.995
PFA $\cdots$ W4	-2.418
W1 $\cdots$ W2	-4.238
W1 $\cdots$ W3	-0.788
W1 $\cdots$ W4	-3.748
W2 $\cdots$ W3	-3.620
W2 $\cdots$ W4	-0.426
W3 $\cdots$ W4	-5.080
total 2-body energy	-37.838
total 2-body energy excluding ref mol	-17.900
PFA $\cdots$ W1 $\cdots$ W2	-2.419
PFA $\cdots$ W1 $\cdots$ W3	-0.310
PFA $\cdots$ W1 $\cdots$ W4	-0.401
PFA $\cdots$ W2 $\cdots$ W3	-1.099
PFA $\cdots$ W2 $\cdots$ W4	-0.214
PFA $\cdots$ W3 $\cdots$ W4	-0.870
W1 $\cdots$ W2 $\cdots$ W3	0.423
W1 $\cdots$ W3 $\cdots$ W4	-0.895
W1 $\cdots$ W2 $\cdots$ W4	0.360
W2 $\cdots$ W3 $\cdots$ W4	-0.793
total 3-body energy	-6.217
total higher (4 and 5)-body energy	0.062
$E_R$	4.719
$\Delta E$	-39.274

<sup>a</sup> The structures chosen are the energetically most favorable structures for each  $n$ . Refer to the text for further details.

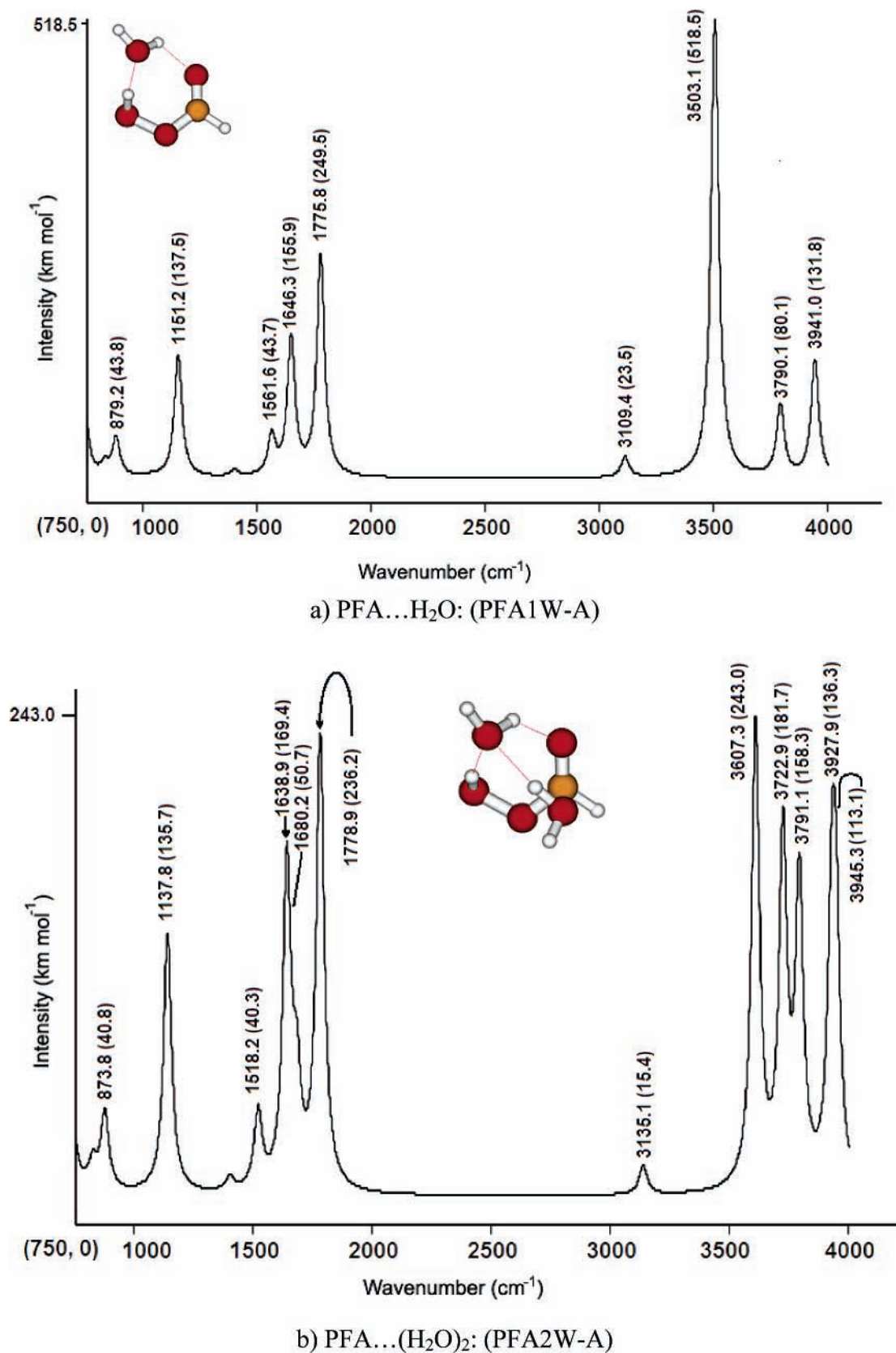
observation is in conformity with the earlier studies on peroxide<sup>23</sup> and water clusters.<sup>24</sup> We have reported only structurally nontrivially distinct clusters; some O–H bond flipped, which turned out, for  $n = 3$ , to be energetically practically degenerate (with the unflipped), structures are not reported in the present study. For the  $n = 4$  case, the O–H bond flipped structures (PFA4W-A to PFA4W-C) are energetically fairly distinct, albeit lying in the narrow interaction energy range between  $-39.289$  and  $-38.895$  kcal mol<sup>-1</sup>.

It should be noted that the structures involving water molecules on the O–O side tend to break the intramolecular hydrogen bond in the PFA molecule (all the structures except

PFA1W-B and PFA1W-C exhibit this feature). Interestingly, addition of water brings in the following restructuring: PFA, which is in cis form, shows a tendency to convert, into trans form by reorientation of the O–H bond out of the plane (of the remainder of the atoms in PFA). Further, if the cluster growth occurs on the opposite side of the O–O bond of PFA, then the resulting structures are expected to show structural patterns similar to those of any carbonyl $\cdots$ H $_2$ O clusters. An attempt has also been made to determine the effect of correlation and basis set on the interaction energy of these clusters. Table 1 summarizes these effects.

It is gratifying that the overall trends in the energetics (cf. Table 1) at the RHF as well as the MP2 level by and large remain consistent. In the present study we also observe that a higher basis set or higher level of theory is accompanied by a decrease in the numerical value of the interaction energy, a fact well documented by several earlier works, including the benchmarking one by Rablen et al.<sup>26</sup> Actually, taking a cue from previous studies, we have chosen the extended basis sets, viz. 6-311++G(2d,2p) (triple- $\zeta$  basis set, augmented with diffuse and polarization functions), to reduce the BSSE to  $\sim 21\%$ . The compactness of the constituent units and the enhanced hydrogen bonding ability of the molecules within the cluster admittedly entail a somewhat higher BSSE. It may be inferred from Table 1 that application of BSSE and zero-point energy (ZPE), individually or in conjunction, invariably lowers the interaction energy. The energy trends do not alter after inclusion of ZPE, albeit its inclusion results in reduction of the interaction energy ( $\Delta E$ ) by  $\sim 27\%$ . Incidentally, it should be noted that the inclusion of both BSSE and ZPE has been reported as an overcorrection.<sup>27</sup>

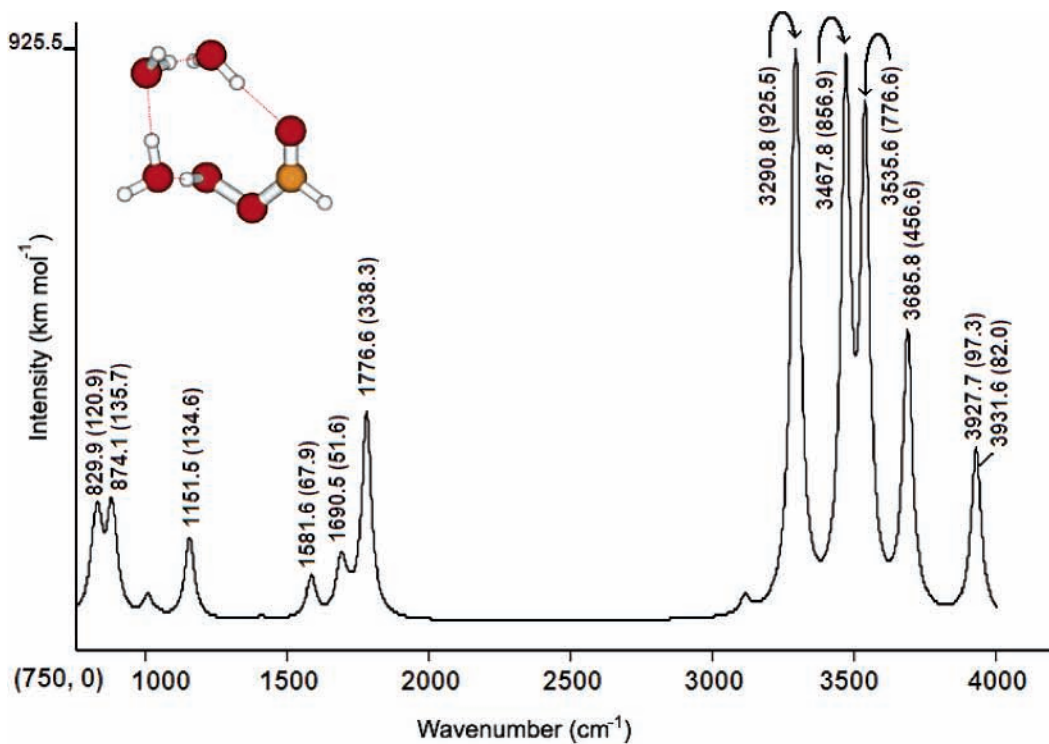
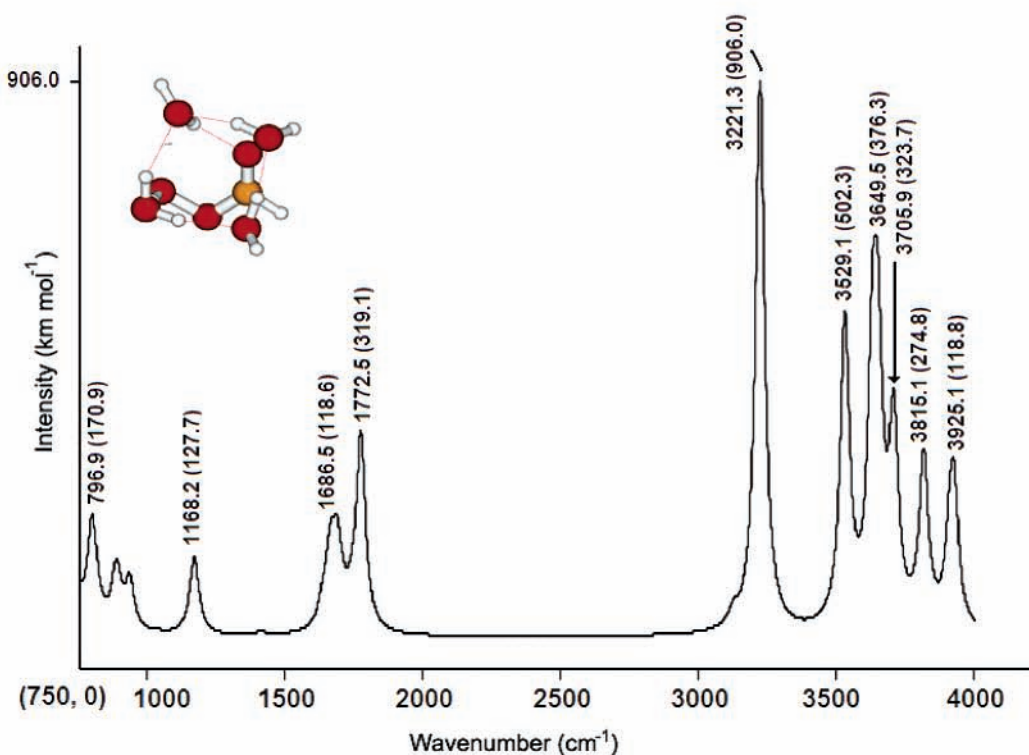
To gauge the strength of individual interactions and quantify the cooperativity in PFA $\cdots$ (H $_2$ O) $_n$  clusters, we have performed many body interaction energy analysis<sup>30–32</sup> employing the MBAC code by Kulkarni and co-workers.<sup>30</sup> The term “body” here implies a molecule (the units of the molecular cluster) taken as a unit. The many body interaction energy analysis has been carried out herein at the MP2/6-311++G(2d,2p) level, for the most favorable structures, viz. PFA2W-A, PFA3W-A, and PFA4W-A. It can be inferred from the MBAC calculations (cf. Table 2) that the attractive component of the interaction energy due to binary pairs, viz. PFA $\cdots$ H $_2$ O and H $_2$ O $\cdots$ H $_2$ O, and ternary pairs, viz. PFA $\cdots$ H $_2$ O $\cdots$ H $_2$ O and H $_2$ O $\cdots$ H $_2$ O $\cdots$ H $_2$ O in the PFA $\cdots$ (H $_2$ O) $_n$  complexes favorably (in terms of stability) leads to an over-binding (more than 100%). For PFA2W-A cluster, two-body interaction energy contributes  $\sim 103\%$  of its interaction energy ( $\Delta E$ ), whereas the proper stability (100%  $\Delta E$ ) is achieved on inclusion of three-body energy terms and cluster relaxation energy ( $E_R$ ). In the case of PFA3W-A, two-body and three-body energy terms together lead to extra stability ( $\sim 103\%$  of its  $\Delta E$ ) and the higher body (four-body) terms and the relaxation energy  $E_R$  together restore the energy to 100%. According to the benchmarking study on many body analysis of water clusters by Xantheas,<sup>32</sup> two- and three-body interactions usually constitute the constructive or additive part of interaction energy whereas higher body terms such as four body, five body, etc. as well as the relaxation energy constitute the repulsive part<sup>23,30</sup> in the interaction energy. The sum total of attractive and repulsive interactions plus relaxation energy is restored to give exactly 100% binding energy. A closer look at the MBAC results indeed provides insights into the binding process. The relaxation energy  $E_R$  per molecule for  $n = 2-4$  cases shows a gradual decrease (for PFA2W-A, 1.303 kcal mol<sup>-1</sup>; for PFA3W-A, 1.127 kcal mol<sup>-1</sup>; for PFA4W-A, 0.944 kcal mol<sup>-1</sup>), which is an indication that the cluster growth will reduce the strain in



**Figure 3.** IR spectra of most favorable cases of (a) PFA...H<sub>2</sub>O (PFA1W-A) and (b) PFA...(H<sub>2</sub>O)<sub>2</sub> (PFA2W-A) clusters simulated at MP2/6-311++G(2d,2p) level.

the molecular system. However, this strain is still higher compared to that estimated for the H<sub>2</sub>O<sub>2</sub>...(H<sub>2</sub>O)<sub>n</sub> systems.<sup>23</sup> A quick comparison shows that the two-body interactions (excluding PFA) in PFA...(H<sub>2</sub>O)<sub>n</sub> and hydrogen peroxide in H<sub>2</sub>O<sub>2</sub>...(H<sub>2</sub>O)<sub>n</sub> clusters follow similar trends. These interactions serve

as a quantitative measure of water...water interactions in the heteroclusters due to the presence of a hetero molecule such as PFA. However, the total two-body interactions in the present case show a stabilization of ~3 kcal mol<sup>-1</sup> or more compared to the parent system, viz. H<sub>2</sub>O<sub>2</sub>...(H<sub>2</sub>O)<sub>n</sub> clusters.

c) PFA...(H<sub>2</sub>O)<sub>3</sub>: (PFA3W-A)d) PFA...(H<sub>2</sub>O)<sub>4</sub>: (PFA4W-A)

**Figure 4.** IR spectra of most favorable cases of (a) PFA...(H<sub>2</sub>O)<sub>3</sub> (PFA3W-A) and (b) PFA...(H<sub>2</sub>O)<sub>4</sub> (PFA4W-A) clusters simulated at MP2/6-311++G(2d,2p) level.

To ensure (local) minimum nature of the energetically favorable structures, vibrational frequency analysis has been performed for all the conformers of PFA...(H<sub>2</sub>O)<sub>*n*</sub> (*n* = 1–4) complexes at the RHF and MP2 levels and sufficiently large basis set used herein. In general PFA...(H<sub>2</sub>O)<sub>*n*</sub>, for *n* > 1, show emergence of additional vibrational levels for the O–H stretch

in water (cf. Figures 3 and 4). The C=O stretch shows a shift to the higher wavenumber side accompanied by modification in the intensity, with increase in the number of water molecules (PFA, 1758.7 (251.8); PFA1W, 1775.8 (249.5); PFA2W, 1778.9 (236.2), 1776.6 (338.3), 1772.5 (319.1) expressed here as cm<sup>-1</sup> (km mol<sup>-1</sup>)). The bending and stretching vibrations in water

molecules and those of PFA show additional vibrational levels with increase in the number of water molecules. Interestingly, the shift to high wavelength (by  $\sim 20 \text{ cm}^{-1}$ ) is also observed for the O–O stretch in PFA. This shift is accompanied by marginal enhancement of intensity. This feature may be attributed to the charge separation brought out by the surrounding water molecules. Figures 3 and 4 show the qualitative IR spectra simulated at the MP2/6-311++G(2d,2p) level for the energetically minimal structures. Actual experimental spectra, on the other hand, will have an admixture of these spectral features due to the response of several energetically comparable conformers.

#### IV. Conclusions

This article represents systematic ab initio investigations of the structure and energetics of  $\text{PFA}\cdots(\text{H}_2\text{O})_n$ , for  $n = 1-4$ ; the best level employed herein is MP2/6-311++G(2d,2p). Interestingly, all the systems bear a close structural resemblance to the  $\text{H}_2\text{O}_2\cdots(\text{H}_2\text{O})_n$  and  $\text{RCOR}'\cdots(\text{H}_2\text{O})_n$  complexes. Enhancing the level of sophistication by the inclusion of correlation, by and large, maintains the trends in the energetics at RHF and MP2 levels with a 6-311++G(2d,2p) basis set. It is expected that accurate experimental data would be required to corroborate the predicted spectral data presented here. At this point it is worthwhile to mention that the energy corrections such as ZPE and BSSE also do not alter the trends in the energetics, although inclusion of these effects lowers the interaction energy of the clusters. As a complementary effect, it is inferred from the many body interaction energy analysis that the PFA $\cdots$ water interaction is stronger than that for water $\cdots$ water or peroxide $\cdots$ water species of the clusters. It is conceivable that, while in its free state in the gaseous phase the cis conformer of PFA is more stable (by  $\sim 2.6 \text{ kcal mol}^{-1}$ )<sup>5</sup> than the trans one, their energy difference, in a solvent with a high dielectric constant, should markedly decrease by virtue of the higher electric dipole moment that the trans conformer possesses (3.62 D) over cis (1.63 D). Such a difference, admittedly, will not be exhibited in their interactions with  $(\text{H}_2\text{O})_n$ , with  $n$  limited to 1–4. The present study, however, may be taken to be a precursor to a possible cis–trans “isomerism”, as indicated by an intramolecular hydrogen bond being replaced by the energetically more favorable hydrogen bonding to the  $\text{H}_2\text{O}$  molecule. Such effects, appropriately described by means of continuum solvation models,<sup>33</sup> would certainly merit a fuller discussion in an independent venture.

The interaction of PFA with water thus brings about changes in its structure, energetics, and binding. Thus, in a description of actual pre-reaction complexes (hydrogen bonded complexes of PFA $\cdots$ water) in aqueous ambience, it is more appropriate to use the present information, rather than that from its vapor-phase environment.

**Acknowledgment.** The authors are thankful to Professor Dr. Shridhar P. Gejji (Department of Chemistry, University of Pune) for several useful discussions and computational help.

#### References and Notes

(1) Bartlett, P. D. *Rec. Chem. Prog.* **1950**, *11*, 47.

- (2) (a) Marinetti, G.; Berry, J. F.; Rouser, G.; Stotz, E. *J. Am. Chem. Soc.* **1953**, *75*, 313. (b) Azman, A.; Koller, J.; Plenicar, B. *J. Am. Chem. Soc.* **1979**, *101*, 1107.
- (3) Oldani, M.; Ha, T. K.; Bauder, A. *J. Am. Chem. Soc.* **1983**, *105*, 360.
- (4) Sanger, F. *Nature* **1947**, *160*, 295.
- (5) Langley, C. H.; Noe, E. A. *THEOCHEM* **2004**, 682, 215.
- (6) Andersen, A.; Carter, E. A. *J. Phys. Chem. A* **2003**, *107*, 9463.
- (7) Okovytyy, S.; Gorb, L.; Leszczynski, J. *Tetrahedron Lett.* **2002**, *43*, 4215.
- (8) Yamabe, S.; Kondou, C.; Minato, T. *J. Org. Chem.* **1996**, *61*, 616.
- (9) Freccero, M.; Gandolfi, R.; Sarzi-Amade, M.; Rastelli, A. *J. Org. Chem.* **2002**, *67*, 8519.
- (10) Bach, R. D.; Canepa, C.; Winter, J. E.; Blanchette, P. E. *J. Org. Chem.* **1997**, *62*, 5191.
- (11) Bach, R. D.; Estevez, C. M.; Winter, J. E.; Glukhovtsev, M. N. *J. Am. Chem. Soc.* **1998**, *120*, 680.
- (12) Cardenas, R.; Cetina, R.; Lagunez-Otero, J.; Reyes, L. *J. Phys. Chem. A* **1997**, *101*, 192.
- (13) Carlo, P. *Chem. Phys.* **1977**, *26*, 243.
- (14) Bach, R. D.; Willis, C. L.; Lang, T. J. *Tetrahedron* **1979**, *35*, 1239.
- (15) Bach, R. D.; Dmitrenko, O. *J. Phys. Chem. A* **2003**, *107*, 4300.
- (16) Bock, C. W.; Trachtman, M.; George, P. *Chem. Phys.* **1981**, *62*, 303.
- (17) Shi, Y.; Zhou, Z. *J. Mol. Struct. (THEOCHEM)* **2004**, *674*, 113.
- (18) Beichert, P.; Schrems, O. *J. Phys. Chem. A* **1998**, *102*, 10540.
- (19) Seinfeld, J. H.; Pandis, S. N. *Atmospheric Chemistry and Physics*; Wiley-Interscience: New York, 1998; pp 249, 356.
- (20) Daza, M. C.; Dobado, J. A.; Molina, J. M.; Villaveces, J. L. *J. Phys. Chem. A* **1999**, *103*, 4755 and references therein.
- (21) Engdahl, A.; Nelander, B.; Karlström, G. *J. Phys. Chem. A* **2001**, *105*, 8393 and references therein.
- (22) Ju, X. H.; Xiao, J. J.; Xiao, H. *J. Mol. Struct. (THEOCHEM)* **2003**, *626*, 231.
- (23) Kulkarni, A. D.; Pathak, R. K.; Bartolotti, L. J. *J. Phys. Chem. A* **2005**, *109*, 4583.
- (24) Maheshwary, S.; Patel, N.; Sathyamurthy, N.; Kulkarni, A. D.; Gadre, S. R. *J. Phys. Chem. A* **2001**, *105*, 10525.
- (25) Frisch, M. J.; Trucks, G. W.; Schlegel, H. B.; Scuseria, G. E.; Robb, M. A.; Cheeseman, J. R.; Montgomery, J. A., Jr.; Vreven, T.; Kudin, K. N.; Burant, J. C.; Millam, J. M.; Iyengar, S. S.; Tomasi, J.; Barone, V.; Mennucci, B.; Cossi, M.; Scalmani, G.; Rega, N.; Petersson, G. A.; Nakatsuji, H.; Hada, M.; Ehara, M.; Toyota, K.; Fukuda, R.; Hasegawa, J.; Ishida, M.; Nakajima, T.; Honda, Y.; Kitao, O.; Nakai, H.; Klene, M.; Li, X.; Knox, J. E.; Hratchian, H. P.; Cross, J. B.; Bakken, V.; Adamo, C.; Jaramillo, J.; Gomperts, R.; Stratmann, R. E.; Yazyev, O.; Austin, A. J.; Cammi, R.; Pomelli, C.; Ochterski, J. W.; Ayala, P. Y.; Morokuma, K.; Voth, G. A.; Salvador, P.; Dannenberg, J. J.; Zakrzewski, V. G.; Dapprich, S.; Daniels, A. D.; Strain, M. C.; Farkas, O.; Malick, D. K.; Rabuck, A. D.; Raghavachari, K.; Foresman, J. B.; Ortiz, J. V.; Cui, Q.; Baboul, A. G.; Clifford, S.; Cioslowski, J.; Stefanov, B. B.; Liu, G.; Liashenko, A.; Piskorz, P.; Komaromi, I.; Martin, R. L.; Fox, D. J.; Keith, T.; Al-Laham, M. A.; Peng, C. Y.; Nanayakkara, A.; Challacombe, M.; Gill, P. M. W.; Johnson, B.; Chen, W.; Wong, M. W.; Gonzalez, C.; Pople, J. A. *Gaussian 03*, revision C.02; Gaussian, Inc.: Wallingford, CT, 2004.
- (26) Rablen, P. R.; Lockman, J. W.; Jorgensen, W. L. *J. Phys. Chem. A* **1998**, *102*, 3782.
- (27) (a) Del Bene, J. E.; Person, W. B.; Szczepaniak, K. *J. Phys. Chem.* **1995**, *99*, 10705. (b) Kim, K.; Jordan, K. D. *J. Phys. Chem.* **1994**, *98*, 10089. (c) Feyereisen, M. W.; Feller, D.; Dixon, D. A. *J. Phys. Chem.* **1996**, *100*, 2993. (d) Laasonen, K.; Parinello, M.; Car, R.; Lee, C.; Vanderbilt, D. *Chem. Phys. Lett.* **1993**, *107*, 107. (e) Lee, C.; Chen, H.; Fitzgerald, G. *J. Chem. Phys.* **1994**, *101*, 4472.
- (28) Limaye, A. C.; Gadre, S. R. Univis-2000: An Indigenously Developed Molecular Visualization Package. *Curr. Sci. (India)* **2001**, *80*, 1296.
- (29) Schaftenaar, G.; Noordik, J. H. MOLDEN: A pre- and post-processing program for molecular and electronic structures. *J. Comput.-Aided Mol. Des.* **2000**, *14*, 123.
- (30) Kulkarni, A. D.; Ganesh, V.; Gadre, S. R. *J. Chem. Phys.* **2004**, *121*, 5043.
- (31) Elrod, M. J.; Saykally, R. J. *Chem. Rev.* **1994**, *94*, 1975.
- (32) Xantheas, S. S. *J. Chem. Phys.* **1994**, *100*, 7532.
- (33) (a) Tomasi, J.; Mennucci, B.; Cammi, R. *Chem. Rev.* **2005**, *105*, 2999. (b) Orozco, M.; Luque, F. J. *Chem. Rev.* **2001**, *101*, 203.